The EMBO Journal (2011) 30, 3430–3441 | © 2011 European Molecular Biology Organization | All Rights Reserved 0261-4189/11
www.embojournal.org

THE EMBO JOURNAL

Developmental regulation of CYCA2s contributes to tissue-specific proliferation in *Arabidopsis*

Steffen Vanneste[1,2,7], Frederik Coppens[1,2,7], EunKyoung Lee[3], Tyler J Donner[4], Zidian Xie[5], Gert Van Isterdael[1,2], Stijn Dhondt[1,2], Freya De Winter[1,2], Bert De Rybel[1,2,8], Marnik Vuylsteke[1,2], Lieven De Veylder[1,2], Jiří Friml[1,2], Dirk Inzé[1,2], Erich Grotewold[5], Enrico Scarpella[4], Fred Sack[3], Gerrit TS Beemster[1,2,6] and Tom Beeckman[1,2,*]

[1]Department of Plant Systems Biology, VIB, Ghent, Belgium, [2]Department of Plant Biotechnology and Bioinformatics, Ghent University, Ghent, Belgium, [3]Department of Botany, University of British Columbia, Vancouver, British Columbia, Canada, [4]Department of Biological Sciences, University of Alberta, Edmonton, Alberta, Canada, [5]Department of Plant Cellular and Molecular Biology and Plant Biotechnology Center, The Ohio State University, Columbus, OH, USA and [6]Department of Biology, University of Antwerp, Antwerp, Belgium

In multicellular organisms, morphogenesis relies on a strict coordination in time and space of cell proliferation and differentiation. In contrast to animals, plant development displays continuous organ formation and adaptive growth responses during their lifespan relying on a tight coordination of cell proliferation. How developmental signals interact with the plant cell-cycle machinery is largely unknown. Here, we characterize plant A2-type cyclins, a small gene family of mitotic cyclins, and show how they contribute to the fine-tuning of local proliferation during plant development. Moreover, the timely repression of *CYCA2;3* expression in newly formed guard cells is shown to require the stomatal transcription factors FOUR LIPS/MYB124 and MYB88, providing a direct link between developmental programming and cell-cycle exit in plants. Thus, transcriptional downregulation of CYCA2s represents a critical mechanism to coordinate proliferation during plant development.

The EMBO Journal (2011) **30,** 3430–3441. doi:10.1038/emboj.2011.240; Published online 19 July 2011
Subject Categories: plant biology
Keywords: A2-type cyclins; differentiation; G2-to-M; proliferation; transcriptional repression

Introduction

After germination, the minimal body plan of the seedling is elaborated by iterative organ development that will shape the adult plant. Each new organ is formed according to a predictable pattern, which reflects a complex interplay between plant hormones and developmental programs (De Veylder *et al*, 2007). One of the targets of morphogenetic cues is the modulation of local cell proliferation and differentiation. Because plant cells cannot move within the plant body due to their rigid cell walls, cell proliferation must be highly controlled in time and space. While recent studies provide insights into the coordination of plant development and cell-cycle regulation, only a few connections between these processes have been identified at the molecular level (Brownfield *et al*, 2009; Sozzani *et al*, 2010; Xie *et al*, 2010).

Cell proliferation is characterized by consecutive cycles of DNA replication (Synthesis; S-phase) and cell division (Mitosis; M-phase). S-phase is preceded by G1-phase, when cells prepare for DNA synthesis, and M-phase by G2-phase, when cells prepare to divide. The orderly transition between phases depends largely on oscillations of Cyclin-Dependent Kinase (CDK) activity. Recently, it was shown that thresholds of CDK activity delineate independent cell-cycle phases (Coudreuse and Nurse, 2010), providing support for a quantitative model of cell-cycle progression. Importantly, CDK activity is modulated at multiple levels. As monomers, CDKs are usually inactive due to a steric blockage of their catalytic cleft. Binding to a cyclin partner removes this block, and thus represents a major regulatory switch of CDK activity (Jeffrey *et al*, 1995). Further fine-tuning of CDK activity is achieved by phosphorylation, dephosphorylation and binding to several cofactors and/or inhibitors (Morgan, 1995, 1997; Inzé and De Veylder, 2006).

Compared with the relatively simple cell-cycle regulatory module in yeast, which includes just one major CDK and a few cyclins (CYC), higher eukaryotes harbour an elaborate repertoire of CDKs and cyclins. Here, the specialized phase- and tissue-specific expression of multiple CDKs and cyclins provides a wide combinatorial range that enables to deal with the increased complexity associated with multicellularity (De Veylder *et al*, 2007; Satyanarayana and Kaldis, 2009).

Animals utilize well-characterized D- and E-type cyclins which are expressed at the onset of cell division (G1-to-S) and which connect extracellular signals with the cell cycle (Matsushime *et al*, 1991; Koff *et al*, 1992; Motokura and Arnold, 1993; Payton and Coats, 2002). Moreover, A- and B-type cyclins are primarily restricted to G2-to-M phase, with A-type cyclins being more broadly expressed, starting as early as S-phase (Pines and Hunter, 1990; Fung and Poon, 2005). Such expression patterns suggest that they function specifically in respective phases of the cell cycle. However, in some cases the loss of one cyclin type can be compensated for by the expression of another cyclin type (Fisher and Nurse, 1996).

*Corresponding author. Department of Plant Systems Biology, VIB, Technologiepark 927, Ghent 9052, Belgium. Tel.: +32 9 331 3930; Fax: +32 9 331 3809; E-mail: tom.beeckman@psb.vib-ugent.be
[7]These authors contributed equally to this work
[8]Present address: Laboratory of Biochemistry, Wageningen University, Wageningen, The Netherlands

Received: 1 February 2011; accepted: 24 June 2011; published online: 19 July 2011

Based on sequence homology and conserved motifs, many core cell-cycle regulators have been annotated in plant genomes (Vandepoele *et al*, 2002). Interestingly, plants have many more cyclins compared with animals. As an example, the *Arabidopsis* genome encodes 10 A-type, 11 B-type and 10 D-type cyclins, but no E-type cyclins, whereas animal genomes usually code for 1 or 2 of each type. In plants, D-type and A3-type cyclins have been implicated in G1-to-S regulation (Dewitte *et al*, 2003, 2007; Takahashi *et al*, 2010), while subgroups of A- and B-type cyclins likely act in G2-to-M regulation (Schnittger *et al*, 2002; Imai *et al*, 2006; Boudolf *et al*, 2009; Ishida *et al*, 2010). The expanded number of cyclins in plants, compared with animals, might represent a mechanism that integrates a broader range of signals to control of proliferation. However, much of what is known about cyclins and plant cell-cycle regulation derives from gain-of-function analyses (Schnittger *et al*, 2002; Dewitte *et al*, 2003; Yu *et al*, 2003; Boudolf *et al*, 2009; Takahashi *et al*, 2010). Quantitative models suggest that the timing of cyclin expression controls differences in cell-cycle regulation (Fisher and Nurse, 1996; Coudreuse and Nurse, 2010), including in plants (Schnittger *et al*, 2002). Therefore, it is essential to define the phenotypic effects of loss of cyclin gene functions to understand their role in plant development.

Although there have been many advances in understanding the regulation of the plant cell cycle, it is still unclear how cell cycling is coordinated with differentiation during development. Components of the G1-to-S transition have been shown to control cell proliferation and differentiation events in shoots (Dewitte *et al*, 2003, 2007) and roots (Wildwater *et al*, 2005; Caro *et al*, 2007; Sozzani *et al*, 2010), which emphasizes the key role of this transition in the cell's decision to exit the cell cycle and activate differentiation. In addition, some differentiated plant cell types are known to undergo multiple rounds of DNA duplication without mitosis (endoreduplication; Melaragno *et al*, 1993), suggesting that cyclin downregulation at the G2-to-M transition could be part of a developmental mechanism that coordinates the switch between proliferation and endoreduplication.

Among putative G2-to-M regulatory cyclins, A2-type cyclins are poorly characterized in plants. In synchronized cell suspensions, their expression starts in S-phase and peaks during the G2-to-M transition (Reichheld *et al*, 1996; Shaul *et al*, 1996; Menges *et al*, 2005). Plant A2 cyclins have been shown to rescue the growth of yeast cyclin-deficient mutants (Setiady *et al*, 1995), and also induced *Xenopus* oocyte maturation (Renaudin *et al*, 1994), suggesting they act during entry into mitosis. Developmentally, CYCA2 expression is not obligately associated with cell proliferation, as it is also expressed in seemingly differentiated cells, such as the vascular tissues (Burssens *et al*, 2000) and developing trichomes (Imai *et al*, 2006). In the vascular tissues, it was proposed that *CYCA2;1* expression reflects a competence to divide, while in trichomes *CYCA2;3* acts to terminate endoreduplication. Indeed, *cyca2;1*, *cyca2;3* and *ilp1-1D* mutants displaying reduced *CYCA2* expression, exhibit increased ploidy levels (Imai *et al*, 2006; Yoshizumi *et al*, 2006), whereas overexpression of *CYCA2;3* shows lower ploidy levels, combined with increased proliferation (Imai *et al*, 2006; Boudolf *et al*, 2009). Recently, auxin signalling has been implicated in the switch from proliferation to endoreduplication as it stimulates *CYCA2;3* expression (Ishida *et al*, 2010). However, it is not clear if this is a direct or indirect effect.

Biochemical interaction studies revealed that plant CYCA2s can interact with a diverse set of CDKs as well as other cell-cycle regulatory proteins (Imai *et al*, 2006; Boudolf *et al*, 2009; Boruc *et al*, 2010b), suggesting that CYCA2s contribute to multiple CDK complexes that might reflect a broad array of biochemical events. Importantly, different CYCA2s have distinct and overlapping expression patterns (Burssens *et al*, 2000; Imai *et al*, 2006) corroborating the idea that tissue-specific co-expression with interaction partners is key to their function. Besides transcriptional regulation, CYCA2s degradation is an equally regulatory mechanism. The Anaphase Promoting Complex (APC) regulates CYCA and CYCB turnover via their destruction boxes (Marrocco *et al*, 2009). Moreover, CCS52A1-dependent activation of the APC mediates proteolysis of CYCA2;3 during the switch to endoreduplication (Boudolf *et al*, 2009). These complex regulatory mechanisms highlight the importance of tight control over the cell cycle.

Here, we address the functional requirement of the subfamily of plant A2-type cyclins in plant cell-cycle regulation in different developmental contexts and report a novel transcriptional repression mechanism that acts during terminal differentiation of guard cells.

Results

Sequence similarity (Vandepoele *et al*, 2002), co-regulation during the cell cycle (Menges *et al*, 2005), subcellular colocalization (Boruc *et al*, 2010a), common interaction partners (Boruc *et al*, 2010b) and mild phenotypes in single mutants (Imai *et al*, 2006; Yoshizumi *et al*, 2006) collectively suggest redundancy among the four CYCA2s in the *Arabidopsis* genome obscuring their functional analysis. To circumvent this obstacle, phenotypic effects of various combinations of multiple *cyca2* loss-of-function mutants were analysed (Supplementary Figure S1).

CYCA2s regulate the G2/M transition in roots

Since CYCA2 expression is strongly associated with proliferative tissues, such as primary and lateral root meristems (Supplementary Figure S2), we probed the impact of their loss-of-function on root growth. Growth defects were apparent when three out of the four *CYCA2*s were mutated. Because the post-embryonic growth of the quadruple mutant was extremely slow, we preferentially analysed triple mutant combinations (Supplementary Figure S3). Triple mutants *cyca2;134* and *cyca2;234* had shorter roots and were impaired in lateral root formation compared with WT (Supplementary Figure S4). To determine whether these growth defects arose from an abnormal cell proliferation, root meristem phenotypes were analysed. Primary root meristems of *cyca2;134* and *cyca2;234* were smaller (Figure 1A; Supplementary Figure S5A and B) and contained fewer dividing cells than WT, as detected by antibodies to the cytokinesis-specific syntaxin KNOLLE (Lauber *et al*, 1997; Figure 1B; Supplementary Figure S5C). Similarly, developing lateral root primordia in *cyca2;234* contained fewer cells than WT (Figure 1C), suggesting that cell proliferation defects underlie both reduced root length and lateral root formation.

To determine at which cell-cycle stage CYCA2s are prominently involved, cell-cycle progression was compared during synchronized lateral root initiation in WT versus *cyca2;234* triple mutants (Figure 1D). In WT, expression of both auxin signalling and G1-to-S regulatory genes preceded the expres-

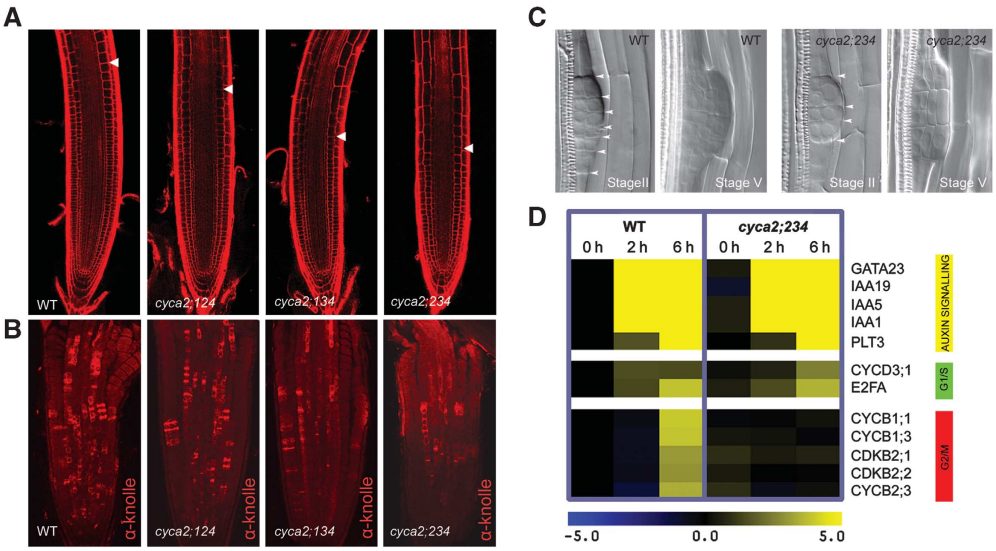

Figure 1 *cyca2* triple mutants have defects in cell-cycle progression. (**A**) Propidium iodide stained root meristems of WT, *cyca2;124 (cyca2;1-1 cyca2;2-1 cyca2;4-1)*, *cyca2;134 (cyca2;1-1 cyca2;3-1 cyca2;4-1)* and *cyca2;234 (cyca2;2-1 cyca2;3-1 cyca2;4-1)* 10 days after germination. Arrowheads indicate the ends of meristems, defined as the position where cells start elongating. (**B**) Immunolocalization of the cytokinesis-specific syntaxin KNOLLE, labelling cells undergoing cytokinesis in roots of 7-day-old WT, *cyca2;124*, *cyca2;134* and *cyca2;234*. (**C**) Stage II and stage V lateral root primordia of WT and *cyca2;234* cleared with chloral hydrate. Lateral root primordia of *cyca2;234* are composed of fewer cells than WT. Arrowheads indicate periclinal cell walls. Stages as defined previously (Malamy and Benfey, 1997). (**D**) Transcriptional responses of auxin signalling genes, G1/S and G2/M regulators in WT and *cyca2;234* root segments during auxin-induced lateral root initiation. In all, 0, 2 and 6 h correspond to time of auxin treatment (10 μM) after being germinated in presence of the auxin transport inhibitor NPA (10 μM). Range indicator from blue to yellow represents expression levels on a $\log_2$ scale relative to NPA germinated WT (0 h).

sion of G2-to-M regulatory genes (Figure 1D), as previously reported (Himanen *et al*, 2002, 2004; Vanneste *et al*, 2005). By contrast, expression of mitotic regulators, such as B-type cyclins, was no longer induced within the same time course in *cyca2;234* mutants, whereas the expression of auxin signalling and G1-to-S regulatory genes was unaffected (Figure 1D). This delay in activation of mitotic regulators indicates that plant CYCA2s function early in the G2/M transition, as was predicted based on sequence homology (Vandepoele *et al*, 2002) and on expression patterns in synchronized cell suspensions (Menges *et al*, 2005). Moreover, it is likely that CYCA2s also function in S-phase, given that CYCA2;2/CDKA;1 can phosphorylate the S-phase regulator E2Fc *in vitro* (del Pozo *et al*, 2002). However, the lack of appropriate markers hampers such determination.

CYCA2s drive proliferation in leaves, while repressing endoreduplication

To obtain its characteristic final size and shape, leaf morphogenesis depends upon a tight coordination between cell proliferation, cell-cycle exit and differentiation. Early leaf development displays high cell division activity that is followed by a gradual tip-to-base deceleration of proliferation and the start of differentiation-associated endoreduplication and cell expansion (Donnelly *et al*, 1999; Beemster *et al*, 2006). The expression pattern of several *CYCA2*s also showed a comparable and dynamic gradient of expression (Supplementary Figure S6; Imai *et al*, 2006). Dramatic increases in ploidy levels and cell sizes were observed in the mature first true leaves of *cyca2* triple mutants (Figure 2A and B). To address the mechanism driving enhanced ploidy levels and cell sizes, the development of *cyca2;234* leaves was analysed in greater detail. Kinematic analysis of leaf growth showed lower cell division rates in *cyca2;234* leaves compared with the WT (Figure 2C; Supplementary Figure S7). In addition, as soon as the first leaf pair became macroscopically visible (after 8 days of growth, Stage 1.02; Boyes *et al*, 2001), DNA content was already dramatically higher than the WT (Figure 2D; %2C, %4C and %8C). Moreover, ploidy levels continued to rise in *cyca2;234* (after 14 days of growth), a period when endoreduplication had already stopped in the WT (Figure 2D; %16C and %32C). Thus, enhanced ploidy levels in *cyca2;234* are the combined result of an early onset and extended duration of endoreduplication. Collectively, these phenotypic and molecular analyses in roots and shoots of *cyca2* triple mutants demonstrate that plant CYCA2s are fundamental elements of the plant cell cycle, and, like their animal counterparts, function in early G2-to-M transition. Furthermore, the enhanced endoreduplication in these mutants is consistent with the observation that low CDK activity allows yeast cells in G2 to (re)enter the G1-to-S program without undergoing mitosis (Coudreuse and Nurse, 2010), suggesting that plant CYCA2s contribute to CDK activities that are required for mitosis.

Tissue-specific CYCA2 expression contributes to vascular proliferation near hydathodes

In addition to their expression in meristems, *CYCA2*s were expressed in the leaf; however, while *CYCA2;2* and *CYCA2;3* were expressed throughout the organ (Supplementary Figures S6, S8 and S9), the expression pattern of *CYCA2;1* and *CYCA2;4* remarkably mimicked the reticulate vein pattern of the leaf (Figure 3A; Supplementary Figure S9). Moreover, the promoter activities of these two genes in the leaf overlapped with one of the earliest hallmarks of the vascular precursor ('preprocambial') cell state (Figure 3B), the promoter activity of the homeodomain-leucine zipper (HD-ZIP) III gene, *ATHB8* (Scarpella *et al*, 2004; Donner *et al*, 2009). The tissue-specific

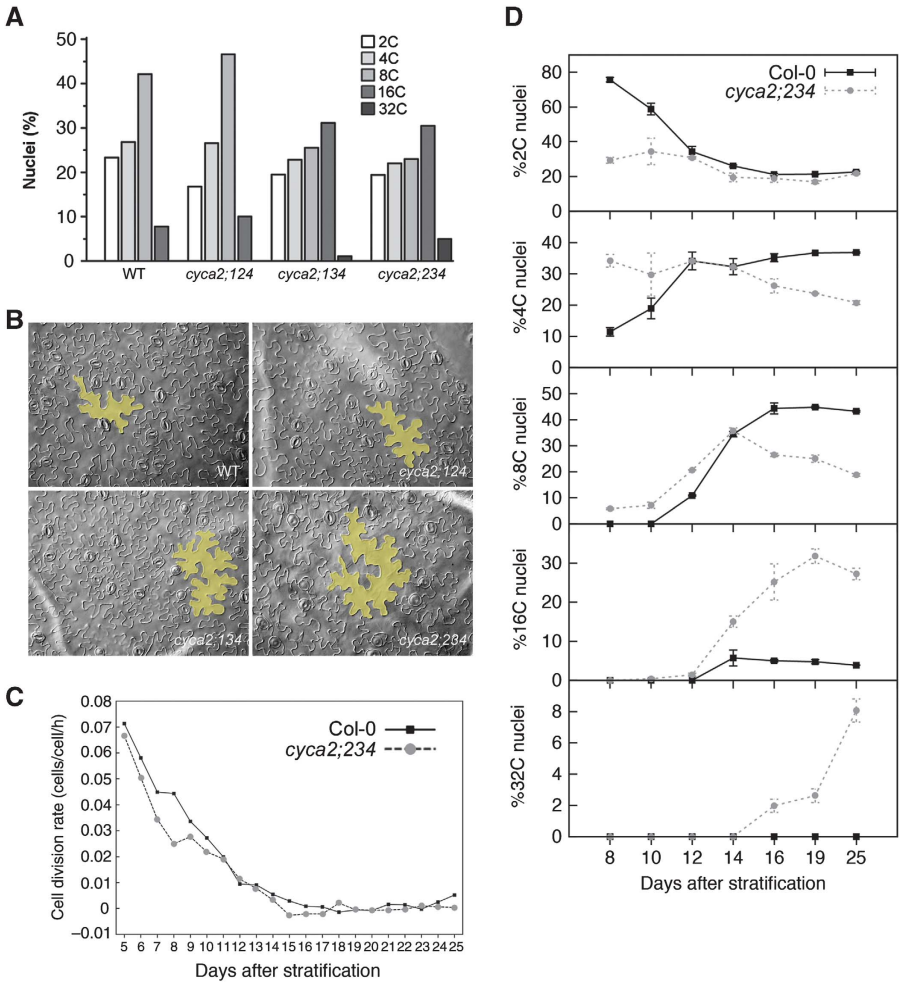

Figure 2 Leaf development shows enhanced endoreduplication and slowed down cell-cycle progression in *cyca2* triple mutants. (**A**) Distribution of nuclear ploidy in mature primary leaves of WT, *cyca2;124*, *cyca2;134* and *cyca2;234*. Triple mutants *cyca2;134* and *cyca2;234* show highest ploidy levels. (**B**) Pavement cell size in mature primary leaves of WT, *cyca2;124*, *cyca2;134* and *cyca2;234*. Yellow overlays highlight representative cells. (**C**) Kinematic analysis reveals a slowdown in cell division rates in developing primary leaves *cyca2;234* compared with WT. (**D**) Evolution of ploidy levels during the development of WT and *cyca2;234* primary leaves. In early stages, WT has predominantly 2C nuclei and a low 4C fraction. Later, the 2C fraction drops rapidly, while higher ploidy fractions increase until ~16 days after stratification. In *cyca2;234*, the 2C fraction is already low at the earliest stage analysed, while the 4C fraction is already high and even a small fraction 8C nuclei can be detected. At later stages, higher ploidy fractions continue to increase, and do not saturate within the time frame of our analysis. Data are represented as mean ± s.e.

expression of *CYCA2;1* and *CYCA2;4* suggests that these *CYCA2* genes function in leaf vascular development. Indeed, *cyca2;234* leaves showed fewer vascular hypertrophy zones than the WT (Figure 3C and D); however, vascular defects in *cyca2;234* were seemingly associated with changes in leaf shape resulting in leaves with fewer serration tips (Figure 3C and E). Additional mutation of the vascular-specific *CYCA2;1* in the *cyca2;234* background further reduced the number of vascular hypertrophy zones without additional effects on the number of serration tips (Figure 3D and E), data which are consistent with the tissue-specific expression pattern of *CYCA2;1*. Thus, vascular cell proliferation defects in *cyca2* mutants likely derive from tissue-specific modulation of *CYCA2* levels, rather than being secondary consequences of disrupted leaf growth.

Stomatal formation requires CYCA2 activity

Stomata consist of two guard cells around a pore whose regulation controls gas exchange between the shoot and the atmosphere. Their development requires at least one asymmetric division as well as a single symmetric division. After the latter division, which occurs in a guard mother cell (GMC) precursor, stomatal differentiation and morphogenesis take place (Bergmann and Sack, 2007). The leaf epidermis of *cyca2;134* and *cyca2;234*, but not those of WT and *cyca2;124*, showed frequent occurrence of unpaired oval cells, displaying cell wall thickenings and plastid accumulations, trait characteristics of wild-type guard cells (Figure 4A). As in normal stomatal guard cells, these single cells were positioned above large intercellular spaces in the subjacent mesophyll (Figure 4B). Moreover, they expressed mature guard cell identity markers, KAT1pro:GUS (Nakamura *et al*, 1995) and ET1728 (Gardner *et al*, 2009; Figure 4C). Thus, these cells correspond to aberrant, single guard cells (SGCs) that are located where stomata would normally be found. These SGCs had twice the nuclear-DNA content (4C) of normal guard cells (2C) (Supplementary Figure S10), suggesting they are arrested in G2-phase. Yet, the aberrant cells

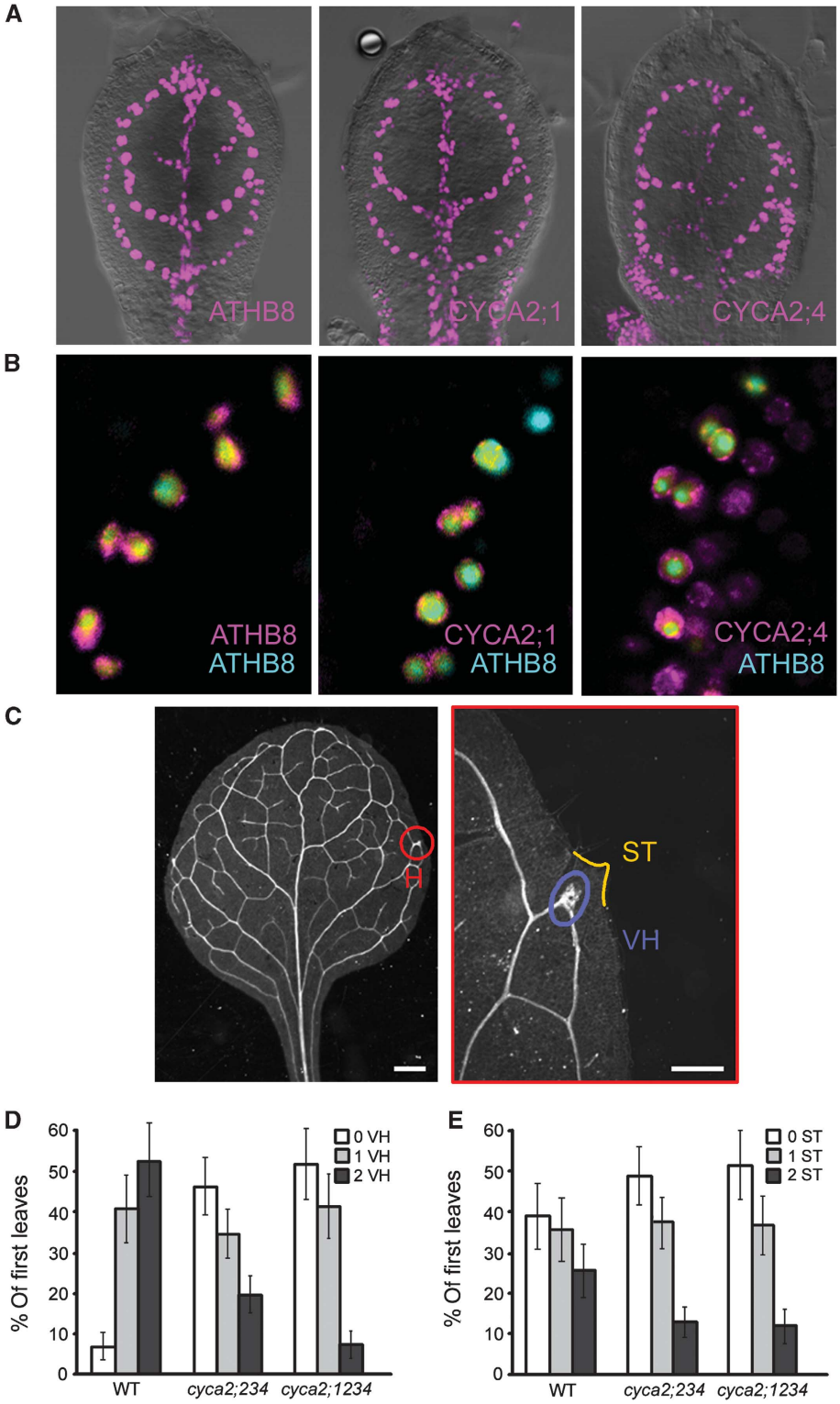

Figure 3 Tissue-specific expression of *CYCA2*s is required for vascular cell proliferation. (**A**) Expression patterns of CYCA2;1pro:HTA6:EYFP and CYCA2;4pro:HTA6:EYFP in 4-DAG first leaves resemble that of ATHB8pro:HTA6:EYFP, which is an early hallmark of vascular development. (**B**) Co-expression of ATHB8pro:HTA6:EYFP, CYCA2;1pro:HTA6:EYFP and CYCA2;4pro:HTA6:EYFP with ATHB8pro:ECFP-Nuc in 4-DAG first leaves. Note how *CYCA2;4* expression is initiated slightly earlier than *ATHB8*, and in wider expression domains that over time narrow to single cell files. In contrast, *CYCA2;1* expression is initiated slightly later than *ATHB8*, but its expression is always confined to single cell files. Images colour-coded with a dual-channel LUT from cyan to magenta through green, yellow and red (Demandolx and Davoust, 1997). Preponderance of cyan signal over colocalized magenta signal is encoded in green, opposite in red and colocalized cyan and magenta signals of equal intensity in yellow. (**C**) Overview of cleared, mature first WT leaf and detail of hydathode (H) that shows vascular hypertrophy (VH) and serration tip (ST). (**D**, **E**) Percentage of mature first leaves showing zero, one or two zones of vascular hypertrophy (VH) (**D**) and serration tips (STs) (**E**). Plots represent mean values ± s.e. Experiments were done in triplicate, and VH and ST were counted on the primary leaves ($19 \leqslant n \leqslant 37$) of each of the three genotypes. A generalized linear model with the multinomial distribution was fitted to the data, as implemented in Genstat (Payne, 2010). VH is significantly affected by genotype ($P = 3.79\text{E}{-11}$), while ST is not ($P = 0.24$).

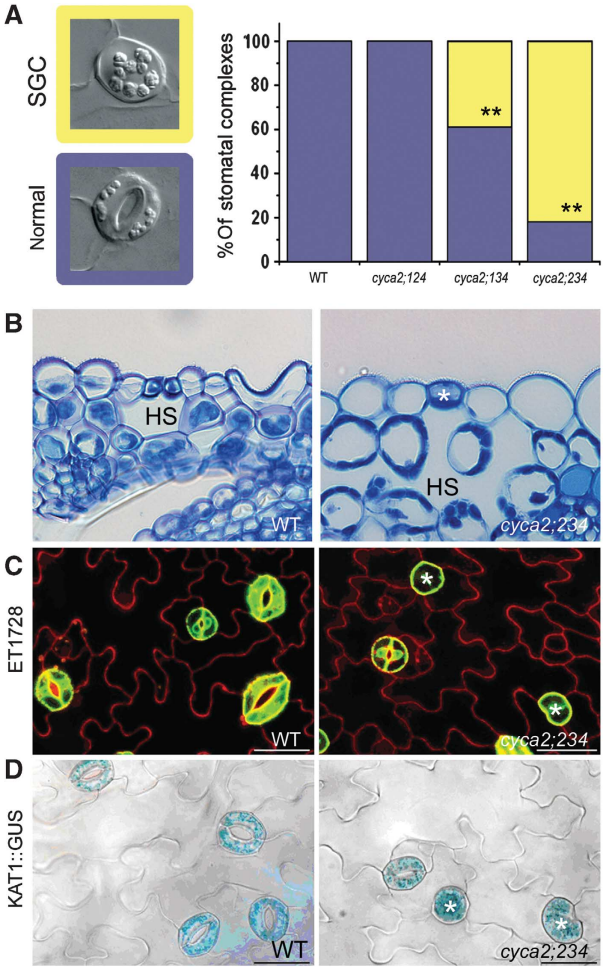

Figure 4 Stomatal expression of *CYCA2*s is required for guard mother cell division. (**A**) Stomatal phenotypes (left) of WT and representative triple mutant. Bar chart: quantification of stomatal phenotypes. Asterisks indicate $P<0.001$; Fisher's exact test (comparison with WT). The *cyca2;234* triple mutant displays the highest frequency of single guard cells (SGCs). Blue = normal stoma; yellow = SGC. (**B**) Anatomical section through a WT stomatal complex and a *cyca2;234* SGC showing correct placement of abnormal SGC (asterisk) over a hypostomatal space (HS). (**C**, **D**) Expression of mature guard cell identity markers; (**C**) ET1728 (GFP) and (**D**) KAT1pro::GUS in WT and *cyca2;234* (asterisks indicate SGCs).

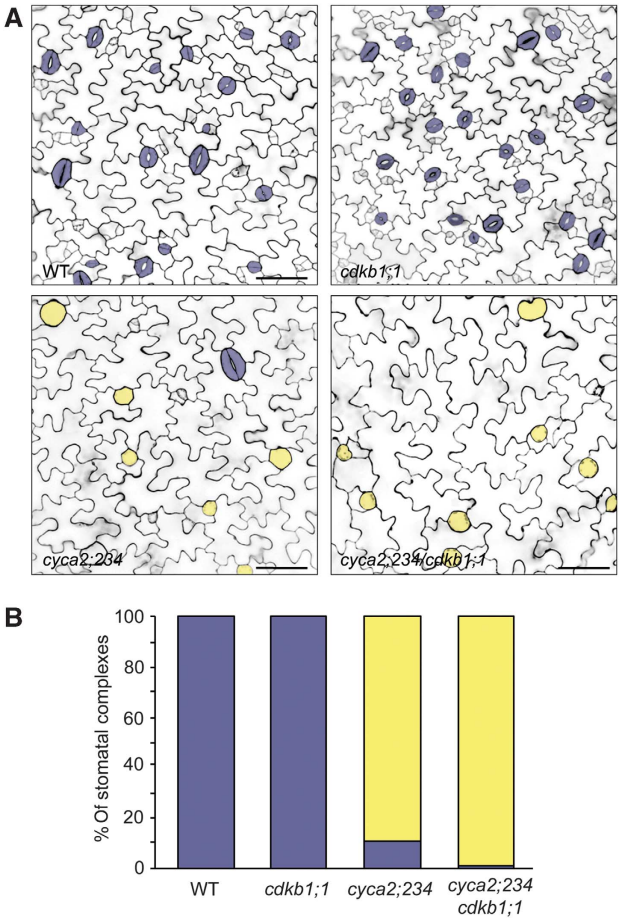

Figure 5 *CYCA2;2, CYCA2;3, CYCA2;4* and *CDKB1;1* genes synergistically promote guard mother cell symmetric division. (**A**) Micrographs of WT, *cdkb1;1, cyca2;234* and quadruple *cyca2;234/cdkb1;1* cotyledons of 4-day-old seedlings. Cell walls in 4-day-old developing cotyledons were visualized using propidium iodide and laser scanning confocal microscopy. False colouring highlights stomatal complexes: blue = normal stoma; yellow = SGC. (**B**) Quantification of stomatal phenotypes. Quadruple *cyca2;234 cdkb1;1* mutant displays more SGCs than *cyca2;234*. (Fisher's exact test, $P=0.0004$).

attained a guard cell identity and formed SGCs instead of a pair.

Strikingly, SGCs could only be found in *cyca2;3* mutant alleles and derived higher order *cyca2* mutant combinations (Supplementary Table SI), suggesting that *CYCA2;3* is a major contributing factor to this phenotype. However, while in single mutants the frequency of SGC formation is very low, additional mutations of other *CYCA2* members resulted in dramatic increases in SGC frequencies (Supplementary Table SI). Collectively, these data demonstrate that CYCA2s are synergistically required for the symmetric division that is a prerequisite for stomatal formation, and that acquisition of guard cell identity occurs independently from GMC division.

CYCA2s and CDKB1s synergistically promote GMC division

SGCs were previously reported in transgenic plants harbouring a *CDKB1;1-N161* dominant-negative construct (Boudolf *et al*, 2004), as well as *cdkb1;1 cdkb1;2* double mutants (Xie *et al*, 2010). Moreover, CDKB1;1 can form a functional complex with CYCA2;3 (Boudolf *et al*, 2009) and *CDKB1;1* is expressed around the time of GMC symmetric division (Boudolf *et al*, 2004), suggesting that CYCA2s and CDKB1s directly interact in promoting the formation of a two-celled stoma. Indeed, while *cdkb1;1* single mutants only had normal stomata, *cyca2;234 cdkb1;1* quadruple mutants displayed even less SGCs than *cyca2;234* triple mutants (Figure 5; Supplementary Figure S11). Thus, all four genes act synergistically in promoting GMC symmetric division, and thus stomatal morphogenesis.

FLP and MYB88 regulate the timely repression of CYCA2;3 *during terminal guard cell differentiation*

While for *CYCA2;1* and *CYCA2;4* no stomatal expression could be observed (Supplementary Figure S12), *CYCA2;3* expression along with *CDKB1;1* and *CYCA2;2*, was induced in late GMCs, remained high in young guard cells, but was strongly reduced or did even disappear in mature stomata

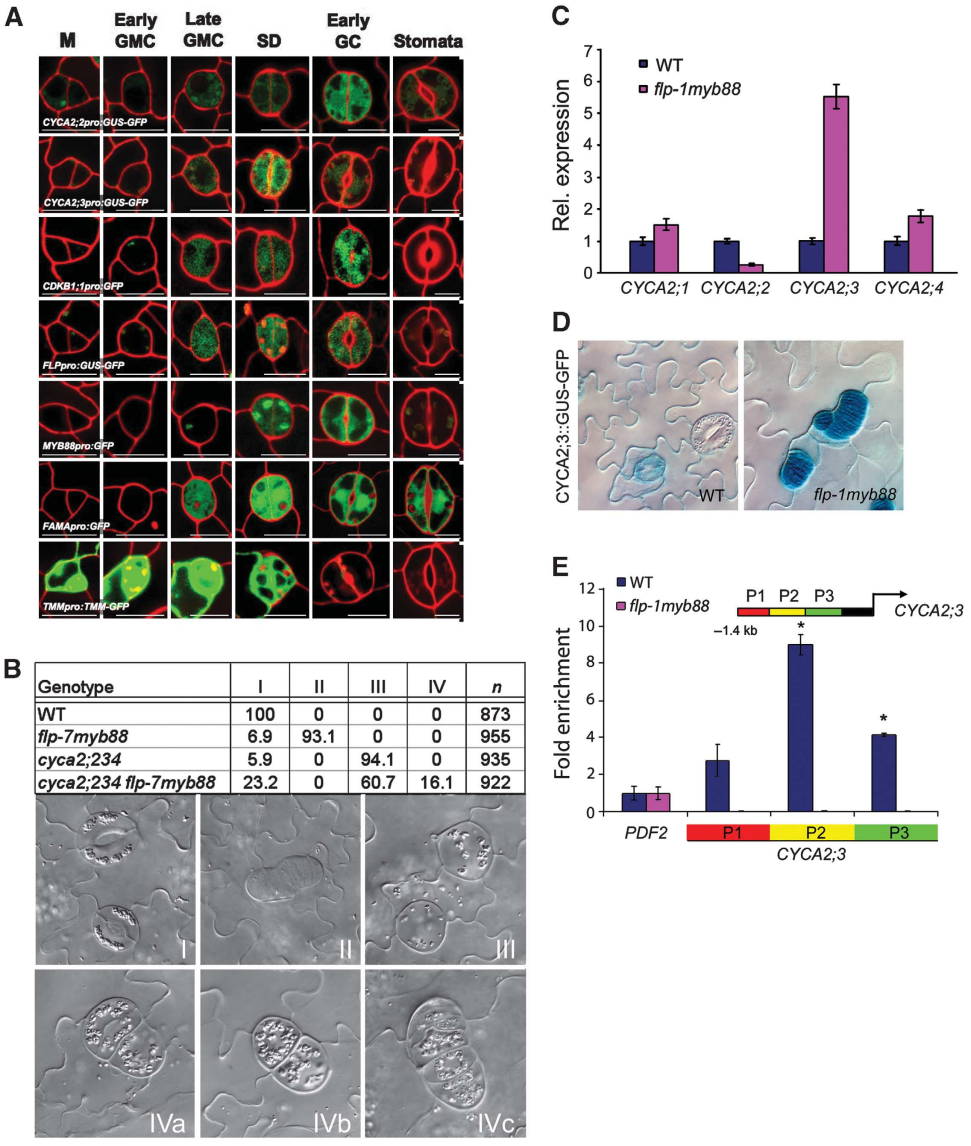

Figure 6 FLP/MYB124 and MYB88 are direct repressors of *CYCA2;3* expression during guard mother cell (GMC) division. (**A**) Expression analysis of transcriptional promoter:reporter fusions (except for TMMpro:TMM:GFP translational fusion). *FLP*, *MYB88* and *FAMA*, which encode transcription factors, are expressed in late GMCs, during symmetric division, and in young guard cells. *TMM* expression marks an earlier phase of stomatal development. *CYCA2;2*, *CYCA2;3* and *CDKB1;1* are expressed at similarly stages to *FLP*, *MYB88* and *FAMA*. Each meristemoid (M) develops into a GMC. Late GMCs have thickened end walls that are usually bisected by the symmetric division (SD) that produces two young guard cells (GCs). The latter undergo further morphogenesis including stomatal pore formation. (**B**) Chart showing frequencies of different stomatal phenotypes in WT, *flp-7 myb88*, *cyca2;234*, and in *cyca2;234 flp-7 myb88*. Stomata in the wild type are normal by definition (type I stomata). In *flp-7 myb88*, many stomata are arranged in clusters (type II), while in *cyca2;234* single guard cells (type III) predominate. In a *cyca2;234 flp-7 myb88* quintuple mutant, most stomata are single-celled (type III), but some small clusters of stomata next to apparent single guard cells are present (type IV), suggesting a 'fusion' phenotype (IVa–c). (**C**) Mean relative expression levels of *CYCA2;1*, *CYCA2;2*, *CYCA2;3*, *CYCA2;4* determined using Q-RT–PCR from cotyledons of WT and *flp-7 myb88* seedlings 10 days after germination. *CYCA2;3* expression in *flp-7 myb88* was markedly higher than in WT (Col-0) (used for reference levels). (**D**) CYCA2;3pro:GUS:GFP in WT and in *flp-1 myb88*. CYCA2;3pro:GUS:GFP GUS levels are low or absent from mature guard cells in WT plants, but is strongly expressed in *flp-1 myb88* stomatal clusters. (**E**) ChIP-Q–PCR on three fragments upstream (−1.4 kb) of the translational start of *CYCA2;3* (P1–P3). PCR conducted on ChIPed DNA samples from 10-day-old wild-type and *flp-1 myb88* shoots using FLP/MYB88 antibody. *PDF2* is a negative control. The positions for PCR products in *CYCA2;3* promoter are indicated. Strongest, specific binding was observed for P2. The error bars indicate the standard error from two biological replicates. Asterisk denotes a statistically significant difference ($P<0.05$).

(Figure 6A). Together with previously identified mutants that have supernumerary guard cells in stomatal complexes (Lai *et al*, 2005; Ohashi-Ito and Bergmann, 2006), the observed decline in cell-cycle gene expression at the end of stomatal development hints at the existence of an active repression mechanism. Loss-of-function mutations in two MYB transcription factors, FOUR LIPS (FLP/MYB124) and its paralogue MYB88 induce clusters of four or more guard cells (Lai *et al*, 2005). Loss-of-function in the basic helix-loop-helix protein FAMA (Ohashi-Ito and Bergmann, 2006) also results in cell clusters, but unlike those of *flp myb88*, without guard cell identity. The apparent independency from the stomata differentiation process renders FLP/MYB124 and MYB88 as potential candidate *CYCA2* repressors, the more because they are

expressed at roughly the same stages of stomatal development as *CYCA2;2*, and *CYCA2;3* (Figure 6A).

To determine whether *CYCA2* expression is required for the extra divisions found in *flpmyb88*, and/or *fama* backgrounds, we generated *cyca2;234 fama-1* quadruple and *cyca2;234 flp-7myb88* quintuple mutants. The *cyca2;234 fama-1* plants did not show any SGCs, instead they formed clusters of cells that lacked guard cell identity; however, these clusters had fewer cells than *fama-1* suggesting that *fama-1* is only partly epistatic to *cyca2;234* (Supplementary Figure S13). By contrast, the formation of stomatal clusters in a *flp-7myb88 cyca2;234* background was completely suppressed (Figure 6B), demonstrating that *CYCA2* gene products are required for the *flp-7myb88* stomatal phenotype and that FLP and MYB88 might represent transcriptional regulators of *CYCA2* expression. Therefore, we analysed *CYCA2* expression in a *flpmyb88* background. Ten days after sowing, cotyledons from *flp-7myb88* seedlings showed about five-fold higher *CYCA2;3* expression than the WT (Figure 6C). Moreover, in *flp-1myb88* stomata, *CYCA2;3* promoter activity remained high after the GMC division (Figure 6D), suggesting that *FLP* and *MYB88* repress *CYCA2;3* promoter activity. To test if this was a direct effect, we performed ChIP-Q-PCR using polyclonal antibodies raised against FLP and MYB88 (Xie *et al*, 2010). In the WT, *CYCA2;3* promoter chromatin fragments were enriched after ChIP, while these were lost in *flp-1myb88* mutants (Figure 6E), demonstrating a specific, direct interaction of FLP and MYB88 with *CYCA2;3* chromatin. Thus, FLP and MYB88 appear to restrict *CYCA2;3* transcription after GMC division via direct interaction with its promoter.

Discussion

CYCA2s modulate the G2-to-M transition

Several findings led to the initial assumption that plant A-type cyclins function in S-phase and in the G2-to-M transition, in analogy to the animal and yeast cell-cycle model. These findings include *CYCA2* expression patterns in synchronized suspension cells (Reichheld *et al*, 1996; Shaul *et al*, 1996; Menges *et al*, 2005), their ability to rescue the growth of yeast cyclin mutants (Setiady *et al*, 1995) and their ability to induce *Xenopus* oocytes maturation (Renaudin *et al*, 1994). In addition, the ectopic expression of plant cyclins is sufficient to drive cells into mitosis (Imai *et al*, 2006; Boudolf *et al*, 2009).

Recently, it was shown that engineered yeast cells arrested in G2 are able to skip mitosis and re-acquire a G1 status when CDK activity is low (Coudreuse and Nurse, 2010). Therefore, if CYCA2s affect mitotic CDK activity, one could expect ectopic endoreduplication and reduced proliferation in the absence of CYCA2 function. Previously, single mutants in *cyca2;1* and *cyca2;3* were shown to have increased levels of endoreduplication (Imai *et al*, 2006; Yoshizumi *et al*, 2006). Consistent with these data, we found that *cyca2* triple mutants displayed greatly increased endoreduplication levels, reduced cell proliferation in developing leaves and G2-arrest of GMCs resulting in SGCs with 4C DNA levels. Together, these data demonstrate that CYCA2s contribute to the CDK activity that is required for mitosis.

In animal systems, it is well established that B-type cyclins in complex with a CDK act as mitosis-promoting factor (MPF). MPF activity is further regulated by A-type cyclins through effects on transcription, activation, localization and stability (Lindqvist *et al*, 2009). In plants, ectopic expression of *CYCB1;2* in differentiated cell types such as trichomes was sufficient to trigger ectopic cell divisions, suggesting a MPF-like function of CYCBs in plants (Schnittger *et al*, 2002). Using an *in planta* synchronized cell cycle-inducible system, we found that the onset of B-type cyclin expression was delayed in *cyca2* triple mutants. Thus, mitotic entry involves the sequential activity of CYCA2-CDK and CYCB-CDK complexes.

Tissue specificity and redundancy among CYCA2s

Each cell type and tissue, within complex organs such as developing leaves, needs a custom-tailored cell-cycle regulation for the organ to reach its typical size and shape. This complexity is reflected in the large number of cell-cycle regulatory genes in plants. In *Arabidopsis*, four *CYCA2* genes are encoded in its genome. Each individual *CYCA2* shows its own peculiar expression patterns across developing organs, displaying tissue- and cell type-specific expression, such as in vascular tissues and the stomatal lineage. Their expression patterns also show variable degrees of overlap in certain tissues, suggesting local redundancies. Striking examples are the vascular expression of *CYCA2;1* and *CYCA2;4* and the stomatal expression of *CYCA2;2* and *CYCA2;3*. In both tissues, the individual genes contribute locally to proliferation in a specific tissue or cell type.

Besides the expression pattern-dependent redundancy, the mutant analyses revealed differential contributions of individual CYCA2s to proliferation. The analysis of the phenotypes of different triple mutants allowed the estimation of their relative importance for specific processes. In the case of root meristem size, lateral root formation, endoreduplication and stomatal development, CYCA2;3 seemed to be most relevant; during stomatal formation, only single *cyca2;3* mutants resulted in SGC formation. Moreover, in combination with *cyca2;3*, other *cyca2* mutations synergistically enhanced the frequency of SGC formation.

Observed differences in penetrance can be explained in part by tissue-specific expression and relative expression levels. However, our study does not allow to exclude effects on protein stability and differences in biochemical properties, as additional regulatory mechanisms.

Developmental control over cell cycle through repression of CYCA2

Proliferation and differentiation are largely mutually exclusive processes. While some cells exit the cell cycle after mitosis and remain in G1-phase, other differentiating cells undergo several rounds of a modified cell cycle, in which the G2-to-M transition is omitted and only DNA synthesis occurs (endoreduplication). In animals, some developmental programs coordinate cell-cycle exit during differentiation through transcription factor activity (Myster and Duronio, 2000; Buttitta and Edgar, 2007). One strategy is to induce CDK inhibitory proteins, while another is to repress cell-cycle activating proteins. Interestingly, the transcription of A-type cyclins is often actively repressed during differentiation processes (Li and Vaessin, 2000; James *et al*, 2006; Martinez *et al*, 2006; Sebastian *et al*, 2009; Pan *et al*, 2010). In plants, it is not known how developmental signals can modulate the switch between a full cell cycle and the endocycle or cell-

cycle exit during differentiation. Previously, increased level of polyploidy1 (ILP1) was found to act as repressor of CYCA2 expression (Yoshizumi *et al*, 2006). Here, we show that FLP and MYB88 repress *CYCA2;3* expression during cell-cycle exit in differentiating guard cells. This mechanism resembles the PROSPERO-dependent mechanism in *Drosophila* that links neuronal lineage development with the transcriptional regulation of cell-cycle regulatory genes (Li and Vaessin, 2000).

Mutations that affect CYCA2 function display higher than normal ploidy levels (Imai *et al*, 2006; Yoshizumi *et al*, 2006), whereas *CYCA2;3* overexpression strongly suppresses endoreduplication (Imai *et al*, 2006; Boudolf *et al*, 2009), indicating that CYCA2 levels are major negative determinants of endoreduplication in leaves. Early stages of leaf development involve high proliferation rates, while later stages gradually switch to differentiation-associated endoreduplication and cell expansion (Donnelly *et al*, 1999; Beemster *et al*, 2006). Interestingly, *CYCA2;3* expression is rapidly repressed during the switch from proliferation to endoreduplication in differentiating leaves (Imai *et al*, 2006). Similarly, antagonizing auxin signalling also enhances endoreduplication via reduced *CYCA2;3* expression (Ishida *et al*, 2010). However, it remains to be seen whether this effect is directly mediated by differentiation-induced transcription factors, and how auxin is involved in this.

Stomatal development ends after a single symmetric division of a GMC, each of whose daughter cells terminally differentiate into individual guard cells (Bergmann and Sack, 2007). Mutants in the stomatal transcription factors FLP and MYB88 do not stop dividing after the GMC has divided, even though guard cell identity markers are expressed (Lai *et al*, 2005). We found that downregulation of *CYCA2;3* after the first GMC division, normally seen in wild-type plant, was absent in *flpmyb88* double mutants. Direct interaction with *CYCA2;3* promoter chromatin corroborate that FLP and MYB88 act as direct repressors of *CYCA2;3* expression in guard cells. Similarly, the expression of an interacting CDK (Boudolf *et al*, 2009; Boruc *et al*, 2010b), *CDKB1;1* was also shown to be directly repressed by FLP and MYB88 (Xie *et al*, 2010). These data are consistent with a model in which FLP and MYB88 enforce cell-cycle exit during terminal guard cell differentiation by direct repression of CYCA2/CDKB1;1 kinase complexes. This mechanism ensures that stomata consist of only two guard cells, a condition required for their proper functioning as adjustable air valves.

Materials and methods

Plant material and growth conditions

We used Arabidopsis seedlings of the accession Col-0 and L*er* and mutants for the various A2-type cyclins from publicly available collections (SALK (Alonso *et al*, 2003), GABI-KAT (Rosso *et al*, 2003) and EXOn Trapping Insert Consortium (EXOTIC; http://www.jic.bbsrc.ac.uk/science/cdb/exotic/index.htm)), and stomatal lineage mutant alleles *flp-1myb88*, *flp-7myb88* (Lai *et al*, 2005) and *fama-1* (Ohashi-Ito and Bergmann, 2006). Cyclin mutant alleles used are *cyca2;1-1* (SALK_121077; Yoshizumi *et al*, 2006), *cyca2;1-2* (SALK_123348), *cyca2;2-1* (GABI_120D03), *cyca2;3-1* (SALK_092515; Imai *et al*, 2006), *cyca2;3-2* (SALK_086463; Imai *et al*, 2006), *cyca2;3-3* (SALK_043246), *cyca2;4-1* (SALK_070301) and *cyca2;4-2* (GAT_5.10009; Supplementary Figure S1). Promoter::reporter lines for FLP (Lai *et al*, 2005), CDKB1;1 (Xie *et al*, 2010) and CYCA2;1 (Burssens *et al*, 2000) have been reported previously. For detection of T-DNA inserts, we used primers specific to the left border of the T-DNAs used for mutagenesis (LBC1, LB_GABI and LB_EXOTIC) in combination with gene-specific primers (Supplementary Table SII). The alleles *cyca2;1-1*, *cyca2;2-1*, *cyca2;3-1* and *cyca2;4-1* are representative knockout alleles and have been used for generating triple mutants. After surface sterilization, seeds were sown on half-strength MS medium supplemented with 1% sucrose and 0.8% agar. After stratification, plates were moved to cooled benches in a growth chamber (temperature, 22°C; irradiation, 65 μE/m^2/s photosynthetically active radiation; photoperiod, 16 h light/8 h dark or continuous light).

Immunofluorescence localization

One-week-old seedlings, grown on 0.5× MS medium under continuous illumination, were fixed in paraformaldehyde. Immunolocalization was performed as described (Sauer *et al*, 2006). The rabbit anti-knolle antibody (1:2000; Lauber *et al*, 1997) and the fluorochrome-conjugated secondary antibody anti-rabbit-Cy3 (1:600; Dianova) were used. Fluorescence detection was done with a confocal laser-scanning microscope Zeiss 710.

Cloning

Promoter::GUS-GFP fusions of MYB88, CYCA2;2, CYCA2;3 and CYCA2;4 were generated through Gateway cloning of promoter fragments into pKGWFS7. PCR fragments of CYCA2;2, CYCA2;3 and CYCA2;4 promoters were described previously (Benhamed *et al*, 2008). To generate the CYCA2;1 and CYCA2;4 transcriptional fusions (CYCA2;1pro:HTA6:EYFP and CYCA2;4pro:HTA6:EYFP, respectively), 1808 bp upstream of the CYCA2;1 start codon and 1963 bp upstream of the CYCA2;4 start codon were amplified from Arabidopsis (*Arabidopsis thaliana*) ecotype Col-0 genomic DNA and cloned into the Gateway-adapted pFYTAG binary vector, which contains a translational fusion between the coding region of histone 2A (HTA6; At5g59870) and that of the enhanced YFP (EYFP) (Zhang *et al*, 2005).

Vascular expression analysis

The origin of the ATHB8pro:HTA6:EYFP and the ATHB8pro:ECFP-Nuc has been described (Sawchuk *et al*, 2007, 2008). Seeds were sterilized and germinated, and seedlings and plants were grown, transformed and selected as described (Sawchuk *et al*, 2007, 2008). For CYCA2;1pro:HTA6:EYFP and CYCA2;4pro:HTA6:EYFP, the progeny of eight independent, single insertion transgenic lines were inspected to identify the most representative expression pattern. We define 'days after germination' (DAG) as days following exposure of imbibed seeds to light. Dissected seedling organs were mounted and imaged as described (Sawchuk *et al*, 2007, 2008; Donner *et al*, 2009). Brightness and contrast were adjusted through linear stretching of the histogram in ImageJ (National Institutes of Health; http://rsb.info.nih.gov/ij). Signal levels and colocalization were visualized as described (Sawchuk *et al*, 2008).

Q-RT–PCR

Total RNA was extracted with the RNeasy Mini kit (Qiagen, Venlo, The Netherlands). Poly(dT) cDNA was prepared from 1 μg total RNA with the Superscript III First Strand Synthesis System for RT–PCR (Invitrogen, Carlsbad, CA) and quantified on an iCycler apparatus (Bio-Rad, Hercules, CA) with the Platinum SYBR Green qPCR Supermix-UDG kit (Invitrogen, Merelbeke, Belgium). PCR was carried out in 96-well optical reaction plates heated for 10 min to 50°C to allow UNG activity, followed by 10 min of 95°C to activate hot start Taq DNA polymerase, and 40 cycles of denaturation for 20 s at 95°C and annealing–extension for 20 s at 58°C. Target quantifications were performed with specific primer pairs designed using Beacon Designer 4.0 (Premier Biosoft International, Palo Alto, CA). Expression levels were normalized to At5g25760 (Q_PEX4) and At4g16100 (Q_UNKN1), which showed constitutive expression across samples. All Q-RT–PCR experiments were performed in triplicates and the data were processed using qBase v1.3.4 (Hellemans *et al*, 2007).

Histochemical staining and anatomical analysis

The β-glucuronidase (GUS) assays were performed as described (Beeckman and Engler, 1994). For microscopic analysis, chlorophyll was removed by EtOH treatment and further cleared by mounting in 90% lactic acid (Acros Organics, Brussels, Belgium). All samples were analysed by differential interference contrast microscopy.

For anatomical sections, samples were fixed overnight in 1% glutaraldehyde and 4% paraformaldehyde in 50 mM phosphate buffer (pH 7). Samples were dehydrated and embedded in

Technovit 7100 resin (Heraeus Kulzer, Wehrheim, Germany) according to the manufacturer's protocol. Sections of 5 μm were cut with a microtome (Minot 1212; Leitz, Wetzlar, Germany), dried on Vectabond-coated object glasses, stained with Toluidine Blue for 8 min (Fluka Chemica, Buchs, Switzerland), and rinsed in tap water for 30 s. After drying, the sections were mounted in DePex medium (British Drug House, Poole, UK).

Flow cytometry

Primary leaves of 3-week-old seedlings were chopped with a razor blade in 300 μl of buffer (45 mM $MgCl_2$, 30 mM sodium citrate, 20 mM 3-[N-morpholino]propanesulphonic acid, pH 7, and 1% Triton X-100). To the supernatants, 1 μl of 4′,6-diamidino-2-phenylindole from a stock of 1 mg/ml was added, which was filtered over a 30-μm mesh. The nuclei were analysed with a CyFlow® ML (Partec) flow cytometer.

Guard cell nuclear content measurement

Nuclei were stained fluorescently by fixing 3-week-old cotyledons in a mixture of 9:1 ethanol:acetic acid (v/v). After the samples had been rinsed, they were stained for 24 h with 0.1 μg/ml of 4′,6-diamidino-2-phenylindole, mounted in Vectashield mounting medium (Vector Laboratories, Burlingame, CA), and observed under a × 63 oil immersion objective on a Zeiss Axioskop equipped with an Axiocam CCD camera (Zeiss). Images were obtained using the Axiovision software and were analysed in grey scale with the public domain image analysis program ImageJ (version 1.28; http://rsb.info.nih.gov/ij/). Relative fluorescence units were reported as integrated density, which are the product of the area and the average fluorescence of the selected nucleus.

Kinematic analysis of leaf development

Plants of the wild-type and the *cyca2* triple mutants were sown in quarter sections of round 12 cm Petri dishes filled with 100 ml of half-strength Murashige and Skoog medium (Duchefa, Haarlem, The Netherlands) and 0.6% plant tissue culture agar (Lab M, Bury, UK). At relevant time points after sowing, plants or primary leaves (depending on the size) of the respective genotypes were harvested. All healthy plants were placed in methanol overnight to remove chlorophyll, and subsequently they were cleared and stored in lactic acid for microscopy.

The following parameters were determined: total area of all cells in the drawing, total number of cells and number of guard cells. From these data, we calculated the average cell area. We estimated the total number of cells per leaf by dividing the leaf area by the average cell area (averaged between the apical and basal positions). Finally, average cell division rates for the whole leaf were determined as the slope of the $\log_2$-transformed number of cells per leaf, which was done using five-point differentiation formulas (Erickson, 1976).

FLP/MYB88 ChIP experiment

Polyclonal antibodies against the FLP/MYB88 proteins were generated by inoculating rabbits with Ni-NTA affinity purified NHis6-MYB88. ChIP experiments were performed essentially as before (Xie *et al*, 2010). In brief, 10-day-old shoots of wild-type, *flp-1 myb88* (200 mg fresh weight for each) were crosslinked in 1% formaldehyde for 20 min by vacuum filtration, and the crosslinking reaction was stopped by the addition of 0.1 M glycine (final concentration) for additional 5 min. Tissues were ground to a fine powder using mortar and pestle in liquid nitrogen and then suspended in 300 μl of lysis buffer (50 mM HEPES, pH 7.5; 150 mM NaCl; 1 mM EDTA, pH 8.0; 1% Triton X-100; 0.1% sodium deoxycholate; 0.1% SDS; 1 mM phenylmethanesulphonylfluoride; 10 mM sodium butyrate; 1 × protein protease inhibitor from Sigma), and sonicated to achieve an average DNA size of 0.3–1 kb. The sonication conditions using the Bioruptor (Diagenode) were as follows: at high power; 30 s of sonication followed by 30 s of break; change ice every 10 min; 30 min in total. After cleared using 30 μl salmon sperm DNA/protein-A agarose (Upstate) at 4°C for at least 1 h, the supernatant fractions were incubated, respectively, with 1 μl FLP/MYB88 rabbit polyclonal antibody or 1 μg rabbit IgG (Abcam) at 4°C overnight. At the same time, 10% of the supernatant was saved as the input fraction. The chromatin–antibody complex was incubated with salmon sperm DNA/protein-A agarose (Upstate) at 4°C for at least 3 h, washed with lysis buffer, LNDET buffer (0.25 M lithium chloride; 1% NP40; 1% sodium deoxycholate and 1 mM EDTA, pH 8.0) and TE buffer (10 mM Tris–Cl, pH 7.5; 1 mM EDTA, pH 8.0) twice, respectively, and the complex was reverse crosslinked in elution buffer (1% SDS; 0.1 M $NaHCO_3$; 1 mg/ml proteinase K) overnight at 65°C. DNA was extracted using the PCR Cleaning Kit (Qiagen). The presence of the promoter of *CYCA2;3* gene was examined by real-time PCR using SYBR-Green chemistry. The housekeeping gene *PDF2/PP2A* (At1g13320) was used as an internal control for normalization. The fold enrichment was normalized to the internal control *PDF2/PP2A* using the $2^{-\Delta\Delta Ct}$ method. Two biological replicates were conducted for each real-time PCR experiment. The ChIP-PCR primers used are listed in Supplementary Table II.

Supplementary data

Supplementary data are available at *The EMBO Journal* Online (http://www.embojournal.org).

Acknowledgements

We thank Dominique Bergmann, David Galbraith and Gerd Jürgens for kindly providing mutant seeds, plasmids and antibodies; Karel Spruyt for assistance with photography; Martine De Cock for help in preparing the manuscript; and NASC for providing T-DNA insertion mutants. The T-DNA mutant GABI_120D03 was generated in the context of the GABI-Kat program and provided by Bernd Weisshaar (MPI for Plant Breeding Research; Cologne, Germany). This work was supported by EMBO and Research Foundation of Flanders grants to SV, by an Excellence Graduate Fellowship from the Plant Molecular Biology/Biotechnology Program at the Ohio State University to ZX, by a National Science Foundation grant to EG and by a Discovery Grant of the Natural Sciences and Engineering Research Council of Canada (NSERC) to ES and FS; ES was supported, in part, by the Canada Research Chairs Program; TJD was supported by an NSERC CGS-M Scholarship, an NSERC CGS-D Scholarship and an Alberta Ingenuity Student Scholarship. SD is indebted to the Agency for Innovation through Science and Technology for a predoctoral fellowship. This work was supported by grants from Ghent University ('Bijzonder Onderzoeksfonds Methusalem project' No. BOF08/01M00408) and the Inter-university Attraction Poles Programme (IUAP VI/33), initiated by the Belgian State, Science Policy Office.

Author contributions: SV, FC, GVI, FD, BDR, JF, GTS and TB conceived the general idea, isolated higher order mutants and performed cell division-related experiments. SD, LDV and DI generated and provided promoter:GUS:GFP lines. TJD and ES conceived and performed vascular-related experiments. SV, EL, FS and TB conceived and performed the stomatal-related experiments. ZX and EG conceived and performed ChIP-PCR. MV performed statistical analyses on the data. SV, FC and TB wrote the paper with input from all authors.

Conflict of interest

The authors declare that they have no conflict of interest.

References

Alonso JM, Stepanova AN, Leisse TJ, Kim CJ, Chen H, Shinn P, Stevenson DK, Zimmerman J, Barajas P, Cheuk R, Gadrinab C, Heller C, Jeske A, Koesema E, Meyers CC, Parker H, Prednis L, Ansari Y, Choy N, Deen H *et al* (2003) Genome-wide insertional mutagenesis of Arabidopsis thaliana. *Science* **301:** 653–657

Beeckman T, Engler G (1994) An easy technique for the clearing of histochemically stained plant tissue. *Plant Mol Biol Rep* **12:** 37–42

Beemster GT, Vercruysse S, De Veylder L, Kuiper M, Inzé D (2006) The Arabidopsis leaf as a model system for investigating the role of cell cycle regulation in organ growth. *J Plant Res* **119:** 43–50

Benhamed M, Martin-Magniette ML, Taconnat L, Bitton F, Servet C, De Clercq R, De Meyer B, Buysschaert C, Rombauts S, Villarroel R, Aubourg S, Beynon J, Bhalerao RP, Coupland G, Gruissem W, Menke FL, Weisshaar B, Renou JP, Zhou DX, Hilson P (2008) Genome-scale Arabidopsis promoter array identifies targets of the histone acetyltransferase GCN5. *Plant J* **56:** 493–504

Bergmann DC, Sack FD (2007) Stomatal development. *Annu Rev Plant Biol* **58:** 163–181

Boruc J, Mylle E, Duda M, De Clercq R, Rombauts S, Geelen D, Hilson P, Inzé D, Van Damme D, Russinova E (2010a) Systematic localization of the Arabidopsis core cell cycle proteins reveals novel cell division complexes. *Plant Physiol* **152:** 553–565

Boruc J, Van den Daele H, Hollunder J, Rombauts S, Mylle E, Hilson P, Inzé D, De Veylder L, Russinova E (2010b) Functional modules in the Arabidopsis core cell cycle binary protein-protein interaction network. *Plant Cell* **22:** 1264–1280

Boudolf V, Barroco R, Engler Jde A, Verkest A, Beeckman T, Naudts M, Inzé D, De Veylder L (2004) B1-type cyclin-dependent kinases are essential for the formation of stomatal complexes in Arabidopsis thaliana. *Plant Cell* **16:** 945–955

Boudolf V, Lammens T, Boruc J, Van Leene J, Van Den Daele H, Maes S, Van Isterdael G, Russinova E, Kondorosi E, Witters E, De Jaeger G, Inzé D, De Veylder L (2009) CDKB1;1 forms a functional complex with CYCA2;3 to suppress endocycle onset. *Plant Physiol* **150:** 1482–1493

Boyes DC, Zayed AM, Ascenzi R, McCaskill AJ, Hoffman NE, Davis KR, Gorlach J (2001) Growth stage-based phenotypic analysis of Arabidopsis: a model for high throughput functional genomics in plants. *Plant Cell* **13:** 1499–1510

Brownfield L, Hafidh S, Borg M, Sidorova A, Mori T, Twell D (2009) A plant germline-specific integrator of sperm specification and cell cycle progression. *PLoS Genet* **5:** e1000430

Burssens S, de Almeida Engler J, Beeckman T, Richard C, Shaul O, Ferreira P, Van Montagu M, Inzé D (2000) Developmental expression of the *Arabidopsis thaliana CYCA2;1* gene. *Planta* **211:** 623–631

Buttitta LA, Edgar BA (2007) Mechanisms controlling cell cycle exit upon terminal differentiation. *Curr Opin Cell Biol* **19:** 697–704

Caro E, Castellano MM, Gutierrez C (2007) A chromatin link that couples cell division to root epidermis patterning in Arabidopsis. *Nature* **447:** 213–217

Coudreuse D, Nurse P (2010) Driving the cell cycle with a minimal CDK control network. *Nature* **468:** 1074–1079

De Veylder L, Beeckman T, Inzé D (2007) The ins and outs of the plant cell cycle. *Nat Rev Mol Cell Biol* **8:** 655–665

del Pozo JC, Boniotti MB, Gutierrez C (2002) *Arabidopsis* E2Fc functions in cell division and is degraded by the ubiquitin-SCF(AtSKP2) pathway in response to light. *Plant Cell* **14:** 3057–3071

Demandolx D, Davoust J (1997) Multicolor analysis and local image correlation in confocal microscopy. *J Microsc* **185:** 21–36

Dewitte W, Riou-Khamlichi C, Scofield S, Healy JM, Jacqmard A, Kilby NJ, Murray JA (2003) Altered cell cycle distribution, hyperplasia, and inhibited differentiation in *Arabidopsis* caused by the D-type cyclin *CYCD3*. *Plant Cell* **15:** 79–92

Dewitte W, Scofield S, Alcasabas AA, Maughan SC, Menges M, Braun N, Collins C, Nieuwland J, Prinsen E, Sundaresan V, Murray JA (2007) Arabidopsis CYCD3 D-type cyclins link cell proliferation and endocycles and are rate-limiting for cytokinin responses. *Proc Natl Acad Sci USA* **104:** 14537–14542

Donnelly PM, Bonetta D, Tsukaya H, Dengler RE, Dengler NG (1999) Cell cycling and cell enlargement in developing leaves of Arabidopsis. *Dev Biol* **215:** 407–419

Donner TJ, Sherr I, Scarpella E (2009) Regulation of preprocambial cell state acquisition by auxin signaling in Arabidopsis leaves. *Development* **136:** 3235–3246

Erickson RO (1976) Modeling of plant growth. *Annu Rev Plant Physiol* **27:** 407–434

Fisher DL, Nurse P (1996) A single fission yeast mitotic cyclin B p34cdc2 kinase promotes both S-phase and mitosis in the absence of G1 cyclins. *EMBO J* **15:** 850–860

Fung TK, Poon RY (2005) A roller coaster ride with the mitotic cyclins. *Semin Cell Dev Biol* **16:** 335–342

Gardner MJ, Baker AJ, Assie JM, Poethig RS, Haseloff JP, Webb AA (2009) GAL4 GFP enhancer trap lines for analysis of stomatal guard cell development and gene expression. *J Exp Bot* **60:** 213–226

Hellemans J, Mortier GR, De Paepe A, Speleman F, Vandesompele J (2007) qBase relative quantification framework and software for management and automated analysis of real-time quantitative PCR data. *Genome Biol* **8:** R19

Himanen K, Boucheron E, Vanneste S, de Almeida Engler J, Inzé D, Beeckman T (2002) Auxin-mediated cell cycle activation during early lateral root initiation. *Plant Cell* **14:** 2339–2351

Himanen K, Vuylsteke M, Vanneste S, Vercruysse S, Boucheron E, Alard P, Chriqui D, Van Montagu M, Inzé D, Beeckman T (2004) Transcript profiling of early lateral root initiation. *Proc Natl Acad Sci USA* **101:** 5146–5151

Imai KK, Ohashi Y, Tsuge T, Yoshizumi T, Matsui M, Oka A, Aoyama T (2006) The A-type cyclin CYCA2;3 is a key regulator of ploidy levels in Arabidopsis endoreduplication. *Plant Cell* **18:** 382–396

Inzé D, De Veylder L (2006) Cell cycle regulation in plant development. *Annu Rev Genet* **40:** 77–105

Ishida T, Adachi S, Yoshimura M, Shimizu K, Umeda M, Sugimoto K (2010) Auxin modulates the transition from the mitotic cycle to the endocycle in Arabidopsis. *Development* **137:** 63–71

James CG, Woods A, Underhill TM, Beier F (2006) The transcription factor ATF3 is upregulated during chondrocyte differentiation and represses cyclin D1 and A gene transcription. *BMC Mol Biol* **7:** 30

Jeffrey PD, Russo AA, Polyak K, Gibbs E, Hurwitz J, Massague J, Pavletich NP (1995) Mechanism of CDK activation revealed by the structure of a cyclinA-CDK2 complex. *Nature* **376:** 313–320

Koff A, Giordano A, Desai D, Yamashita K, Harper JW, Elledge S, Nishimoto T, Morgan DO, Franza BR, Roberts JM (1992) Formation and activation of a cyclin E-cdk2 complex during the G1 phase of the human cell cycle. *Science* **257:** 1689–1694

Lai LB, Nadeau JA, Lucas J, Lee EK, Nakagawa T, Zhao L, Geisler M, Sack FD (2005) The Arabidopsis R2R3 MYB proteins FOUR LIPS and MYB88 restrict divisions late in the stomatal cell lineage. *Plant Cell* **17:** 2754–2767

Lauber MH, Waizenegger I, Steinmann T, Schwarz H, Mayer U, Hwang I, Lukowitz W, Jürgens G (1997) The Arabidopsis KNOLLE protein is a cytokinesis-specific syntaxin. *J Cell Biol* **139:** 1485–1493

Li L, Vaessin H (2000) Pan-neural Prospero terminates cell proliferation during Drosophila neurogenesis. *Genes Dev* **14:** 147–151

Lindqvist A, Rodriguez-Bravo V, Medema RH (2009) The decision to enter mitosis: feedback and redundancy in the mitotic entry network. *J Cell Biol* **185:** 193–202

Malamy JE, Benfey PN (1997) Organization and cell differentiation in lateral roots of *Arabidopsis thaliana*. *Development* **124:** 33–44

Marrocco K, Thomann A, Parmentier Y, Genschik P, Criqui MC (2009) The APC/C E3 ligase remains active in most post-mitotic Arabidopsis cells and is required for proper vasculature development and organization. *Development* **136:** 1475–1485

Martinez AM, Colomb S, Dejardin J, Bantignies F, Cavalli G (2006) Polycomb group-dependent Cyclin A repression in Drosophila. *Genes Dev* **20:** 501–513

Matsushime H, Roussel MF, Ashmun RA, Sherr CJ (1991) Colony-stimulating factor 1 regulates novel cyclins during the G1 phase of the cell cycle. *Cell* **65:** 701–713

Melaragno JE, Mehrotra B, Coleman AW (1993) Relationship between endopolyploidy and cell size in epidermal tissue of Arabidopsis. *Plant Cell* **5:** 1661–1668

Menges M, de Jager SM, Gruissem W, Murray JA (2005) Global analysis of the core cell cycle regulators of Arabidopsis identifies novel genes, reveals multiple and highly specific profiles of expression and provides a coherent model for plant cell cycle control. *Plant J* **41:** 546–566

Morgan DO (1995) Principles of CDK regulation. *Nature* **374:** 131–134

Morgan DO (1997) Cyclin-dependent kinases: engines, clocks, and microprocessors. *Annu Rev Cell Dev Biol* **13:** 261–291

Motokura T, Arnold A (1993) Cyclin D and oncogenesis. *Curr Opin Genet Dev* **3:** 5–10

Myster DL, Duronio RJ (2000) To differentiate or not to differentiate? *Curr Biol* **10:** R302–R304

Nakamura RL, McKendree Jr WL, Hirsch RE, Sedbrook JC, Gaber RF, Sussman MR (1995) Expression of an Arabidopsis potassium channel gene in guard cells. *Plant Physiol* **109:** 371–374

Ohashi-Ito K, Bergmann DC (2006) Arabidopsis FAMA controls the final proliferation/differentiation switch during stomatal development. *Plant Cell* **18:** 2493–2505

Pan J, Nakade K, Huang YC, Zhu ZW, Masuzaki S, Hasegawa H, Murata T, Yoshiki A, Yamaguchi N, Lee CH, Yang WC, Tsai EM, Obata Y, Yokoyama KK (2010) Suppression of cell-cycle progression by Jun dimerization protein-2 (JDP2) involves downregulation of cyclin-A2. *Oncogene* **29:** 6245–6256

Payne RW (2010) *Genstat Release 13 Reference Manual, Part3: Procedure Library PL21*. VSN International: Oxford, UK

Payton M, Coats S (2002) Cyclin E2, the cycle continues. *Int J Biochem Cell Biol* **34:** 315–320

Pines J, Hunter T (1990) Human cyclin A is adenovirus E1A-associated protein p60 and behaves differently from cyclin B. *Nature* **346:** 760–763

Reichheld JP, Chaubet N, Shen WH, Renaudin JP, Gigot C (1996) Multiple A-type cyclins express sequentially during the cell cycle in Nicotiana tabacum BY2 cells. *Proc Natl Acad Sci USA* **93:** 13819–13824

Renaudin JP, Colasanti J, Rime H, Yuan Z, Sundaresan V (1994) Cloning of four cyclins from maize indicates that higher plants have three structurally distinct groups of mitotic cyclins. *Proc Natl Acad Sci USA* **91:** 7375–7379

Rosso MG, Li Y, Strizhov N, Reiss B, Dekker K, Weisshaar B (2003) An Arabidopsis thaliana T-DNA mutagenized population (GABI-Kat) for flanking sequence tag-based reverse genetics. *Plant Mol Biol* **53:** 247–259

Satyanarayana A, Kaldis P (2009) Mammalian cell-cycle regulation: several Cdks, numerous cyclins and diverse compensatory mechanisms. *Oncogene* **28:** 2925–2939

Sauer M, Paciorek T, Benková E, Friml J (2006) Immunocytochemical techniques for whole-mount in situ protein localization in plants. *Nat Protoc* **1:** 98–103

Sawchuk MG, Donner TJ, Head P, Scarpella E (2008) Unique and overlapping expression patterns among members of photosynthesis-associated nuclear gene families in Arabidopsis. *Plant Physiol* **148:** 1908–1924

Sawchuk MG, Head P, Donner TJ, Scarpella E (2007) Time-lapse imaging of Arabidopsis leaf development shows dynamic patterns of procambium formation. *New Phytol* **176:** 560–571

Scarpella E, Francis P, Berleth T (2004) Stage-specific markers define early steps of procambium development in Arabidopsis leaves and correlate termination of vein formation with mesophyll differentiation. *Development* **131:** 3445–3455

Schnittger A, Schobinger U, Stierhof YD, Hulskamp M (2002) Ectopic B-type cyclin expression induces mitotic cycles in endoreduplicating *Arabidopsis* trichomes. *Curr Biol* **12:** 415–420

Sebastian S, Sreenivas P, Sambasivan R, Cheedipudi S, Kandalla P, Pavlath GK, Dhawan J (2009) MLL5, a trithorax homolog, indirectly regulates H3K4 methylation, represses cyclin A2 expression, and promotes myogenic differentiation. *Proc Natl Acad Sci USA* **106:** 4719–4724

Setiady YY, Sekine M, Hariguchi N, Yamamoto T, Kouchi H, Shinmyo A (1995) Tobacco mitotic cyclins: cloning, characterization, gene expression and functional assay. *Plant J* **8:** 949–957

Shaul O, Mironov V, Burssens S, Van Montagu M, Inze D (1996) Two Arabidopsis cyclin promoters mediate distinctive transcriptional oscillation in synchronized tobacco BY-2 cells. *Proc Natl Acad Sci USA* **93:** 4868–4872

Sozzani R, Cui H, Moreno-Risueno MA, Busch W, Van Norman JM, Vernoux T, Brady SM, Dewitte W, Murray JA, Benfey PN (2010) Spatiotemporal regulation of cell-cycle genes by SHORTROOT links patterning and growth. *Nature* **466:** 128–132

Takahashi I, Kojima S, Sakaguchi N, Umeda-Hara C, Umeda M (2010) Two Arabidopsis cyclin A3s possess G1 cyclin-like features. *Plant Cell Rep* **29:** 307–315

Vandepoele K, Raes J, De Veylder L, Rouze P, Rombauts S, Inzé D (2002) Genome-wide analysis of core cell cycle genes in *Arabidopsis*. *Plant Cell* **14:** 903–916

Vanneste S, De Rybel B, Beemster GT, Ljung K, De Smet I, Van Isterdael G, Naudts M, Iida R, Gruissem W, Tasaka M, Inzé D, Fukaki H, Beeckman T (2005) Cell cycle progression in the pericycle is not sufficient for SOLITARY ROOT/IAA14-mediated lateral root initiation in Arabidopsis thaliana. *Plant Cell* **17:** 3035–3050

Wildwater M, Campilho A, Perez-Perez JM, Heidstra R, Blilou I, Korthout H, Chatterjee J, Mariconti L, Gruissem W, Scheres B (2005) The RETINOBLASTOMA-RELATED gene regulates stem cell maintenance in Arabidopsis roots. *Cell* **123:** 1337–1349

Xie Z, Lee E, Lucas JR, Morohashi K, Li D, Murray JA, Sack FD, Grotewold E (2010) Regulation of cell proliferation in the stomatal lineage by the Arabidopsis MYB FOUR LIPS via direct targeting of core cell cycle genes. *Plant Cell* **22:** 2306–2321

Yoshizumi T, Tsumoto Y, Takiguchi T, Nagata N, Yamamoto YY, Kawashima M, Ichikawa T, Nakazawa M, Yamamoto N, Matsui M (2006) Increased level of polyploidy1, a conserved repressor of CYCLINA2 transcription, controls endoreduplication in Arabidopsis. *Plant Cell* **18:** 2452–2468

Yu Y, Steinmetz A, Meyer D, Brown S, Shen WH (2003) The tobacco A-type cyclin, *Nicta;CYCA3;2*, at the nexus of cell division and differentiation. *Plant Cell* **15:** 2763–2777

Zhang C, Gong FC, Lambert GM, Galbraith DW (2005) Cell type-specific characterization of nuclear DNA contents within complex tissues and organs. *Plant Methods* **1:** 7